Alanine Radicals. 2. The Composite Polycrystalline Alanine EPR Spectrum Studied by ENDOR, Thermal Annealing, and Spectrum Simulations†

ARTICLE *in* THE JOURNAL OF PHYSICAL CHEMISTRY A · AUGUST 2002

Impact Factor: 2.69 · DOI: 10.1021/jp026023c

4 AUTHORS, INCLUDING:

Eli Olaug Hole
University of Oslo
85 PUBLICATIONS **1,478** CITATIONS
SEE PROFILE

Einar Sagstuen
University of Oslo
176 PUBLICATIONS **2,393** CITATIONS
SEE PROFILE

Alanine Radicals. 2. The Composite Polycrystalline Alanine EPR Spectrum Studied by ENDOR, Thermal Annealing, and Spectrum Simulations†

Mojgan Z. Heydari, Eirik Malinen, Eli O. Hole, and Einar Sagstuen*

Department of Physics, University of Oslo, P.O. Box 1048 Blindern, N-0316 Oslo 3, Norway

Received: April 26, 2002; In Final Form: July 1, 2002

Radiation-induced free radical formation in the amino acid *l*-α-alanine has been studied using powder and single-crystal X-, K-, and Q-band electron paramagnetic resonance (EPR) spectroscopy, X-band powder electron−nuclear double resonance (ENDOR), thermal annealing, and EPR spectrum simulations. The spectra obtained after room temperature irradiations are composite, consisting of resonances from mainly three radicals denoted **R1**, **R2**, and **R3**. **R1** is the well-known, stable room-temperature species formed by deamination from a protonated alanine anion radical. On the basis of simulations of EPR spectra obtained at X-, K-, and Q-bands, the room-temperature EPR spectrum seems to consist of about 55% of **R1**. Upon thermal annealing, the **R1** resonance disappears faster than those of the other two components. The **R2** species is presumably formed in the oxidative chain of radiation-induced events by net H-abstraction from the central alanine carbon atom. Q-band EPR was used to determine the *g*-tensor of **R2**. This species contributes about 35% to the resonance recorded at room temperature. Upon thermal annealing this radical decays slower than **R1**, resulting in the predominance of **R2** in spectra obtained after prolonged warming at 480 K. Powder ENDOR was used to verify that the dominating species remaining after thermal annealing at this temperature indeed is **R2** and not a successor species of either of the room-temperature radicals. The **R3** species was previously assigned to an N-deprotonated version of **R2** being additionally protonated at the carboxyl group. Detailed spectral data for this resonance are missing but a set of parameters based on available data and otherwise estimated using literature values for similar products was constructed. Simulations indicated that 5−10% of the room-temperature resonance could be ascribed to **R3**. **R3** is more heat-resistant than the **R1** and **R2** radicals, and after prolonged annealing at 480K it was estimated that the resulting resonance consisted of about 51% **R2** and 43% **R3**. The remaining part (about 6%) of the resonance was due to **R1**. These numbers must, however, be considered as tentative because of the lack of precise spectral data for **R3**.

1. Introduction

The simple amino acid *l*-α-alanine (see structure below) has attained considerable interest for use in radiation dosimetry[1−4] and has been formally accepted as a secondary standard for high-dose and transfer dosimetry. The electron paramagnetic resonance (EPR) powder spectrum from amorphous alanine pellets or other types of polycrystalline alanine samples have been used for this purpose. Figure 1a shows a typical example of such an EPR spectrum. The amplitude of the central line of this powder spectrum readout is usually used for monitoring the radiation dose.

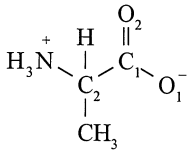

l-α-alanine

For many years, it was assumed that the polycrystalline EPR spectrum from irradiated alanine mainly is due to only one single radiation-induced radical. This species, radical **R1**, often called the SAR, *s*table *a*lanine *r*adical (see Structure 1 below), is formed by deamination from a protonated alanine radical anion.[5−8]

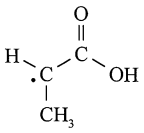

Structure 1
R1 (SAR)

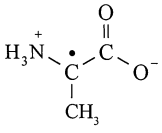

Structure 2
R2

In Figure 1, the EPR spectrum from an alanine pellet X-irradiated at room temperature (a) is compared with the spectrum from a polycrystalline sample of partially deuterated alanine (b). As indicated by the dotted lines, the extreme outer features of the regular spectrum from nondeuterated alanine are missing from the spectrum of the deuterated sample. This observation differs from that mentioned by Arber et al.[8] However, this observation is the most compelling evidence obtained from polycrystalline spectra that the standard alanine spectrum consists of a resonance in addition to that from the **R1** radical because **R1** contains no exchangeable protons.

In two recent papers we have shown that in single crystals of alanine at least three different radicals are formed and stabilized at room temperature.[9,10] Two of these, the **R1** radical

† Part 1: Sagstuen, E.; Hole, E. O.; Haugedal, S. R.; Nelson, W. H. *J. Phys. Chem. A* **1997**, *101*, 9763.

* Corresponding author: Department of Physics, University of Oslo, P.O. Box 1048 Blindern, N-0316 Oslo, Norway. E-mail: einar.sagstuen@fys.uio.no.

10.1021/jp026023c CCC: $22.00
Published on Web 08/28/2002

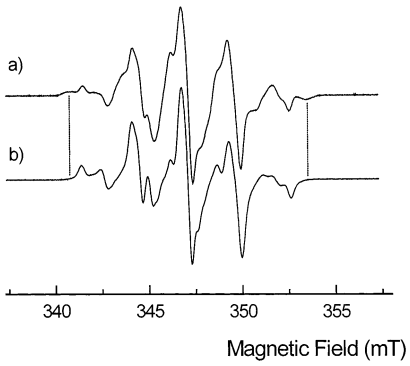

Figure 1. First derivative X-band EPR spectra from polycrystalline *l*-α-alanine X-irradiated and measured at 295 K. Each spectrum is centered at $g = 2.0023$. (a) Nondeuterated sample, dose = 6.4 kGy. (b) Deuterated sample, dose = 7 kGy. Dotted lines indicate spectral features specific for the **R2** radical, features not present in the partially deuterated sample.

(SAR, Structure 1) and a species (radical **R2**, Structure 2) formed by net hydrogen abstraction from the central carbon atom, seem to occur in comparable relative amounts. The third species (denoted **R3**) apparently is a minority species and an unambiguous structure assignment has not yet been made.[9] Structure 3 below was suggested, however, as a possible candidate for **R3**. Whereas **R1** is assumed to be a species formed in the reductive chain of radiation-induced events, **R2** and **R3** are both most probably oxidation products.[9,11,12]

Any satisfactory computer reconstruction of the polycrystalline EPR spectra of alanine consequently should include the resonances from these two additional radical species, with parameters extracted from single-crystal experiments where available.[9]

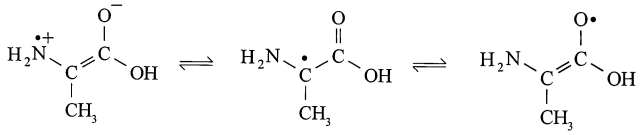

Structure 3

R3

Recently, several groups have made density functional theory-based (DFT) molecular orbital calculations on possible radicals formed from alanine.[11−15] The results from these calculations agree very well with each other and with available experimental single-crystal data,[9] and together they provide substantial support to the structural interpretation of the three radicals in alanine as outlined above.

Several groups have also recently reported that by warming irradiated alanine to above 460 K the EPR spectra change irreversibly (Ciesielski, B., private communication, 2001).[16] The resonance remaining after the almost complete disappearance of **R1** also seems to be similar to that observed by Wieser et al.[17] after long-term UV-irradiation of an irradiated alanine sample. Vanhaelewyn et al. suggested that the remaining pattern mainly consists of the resonance due to **R2**.[16]

The major purpose of the present work is to show by powder electron−nuclear double-resonance (ENDOR) spectroscopy that the high-temperature resonance from alanine has a significant contribution from both the **R2** and **R3** radicals. Furthermore, by spectrum simulations it will be shown that the experimental polycrystalline alanine spectra at room temperature, as well as after warming, are reproduced in a satisfactory manner using the EPR parameters measured or estimated (for **R3**) for the three major radicals in alanine.

2. Methods

Polycrystalline samples of *l*-α-alanine were obtained from Sigma-Aldrich and used without further purification. Single crystals were obtained by slow evaporation from aqueous solutions at room temperature. Partially deuterated crystals were obtained similarly by repeated recrystallizations from 99% D_2O. The crystals are orthorhombic with space group $P2_12_12_1$.[18] Crystals were oriented and mounted for EPR and ENDOR measurements using X-ray diffraction methods to ascertain correct orientations, as described earlier.[9] Pellets were pressed from the commercial polycrystalline samples using a 5-mm Weber pellet press. Irradiations were performed using a Phillips side-window X-ray tube operating at 60 kV and 40 mA. Crystals were given doses of about 30 kGy, powders and pellets as specified below. For heating irradiated powder (polycrystalline) samples before EPR measurements, a THERMOLYNE 1300 furnace was used, equipped with a calibrated thermostated heater. A thin layer of irradiated alanine powder on an aluminum foil sheet was placed in the oven for predetermined times. The air temperature in the oven was continuously monitored. After removal from the oven and cooling to room temperature, pellets were pressed from the powder without the addition of any binder material.

EPR/ENDOR spectra were recorded with a Bruker ESP300E spectrometer equipped with standard X- and Q-band bridges. For X-band EPR, a dual cavity was used with a Mn^{2+}/MgO reference sample (JEOL Co.) permanently mounted in the second cavity. For X-band ENDOR, the Bruker ENDOR cavity and the DICE ENDOR accessory were used together with an ENI 3200L 200-W radiofrequency amplifier. For variable temperature measurements, a Bruker ER 4111 Variable temperature accessory was used. Q-band EPR was performed with a homemade cylindrical Q-band cavity including a permanently mounted Mn^{2+}/MgO reference sample. Microwave frequencies were monitored using a HP 53152A frequency counter/power meter operating in the range 10 Hz to 46 GHz. In all EPR experiments the microwave power was kept below 0.5 mW to avoid power-saturation phenomena and any unnecessary influence of forbidden transitions and spin-flip lines.[9,10] Similarly, modulation amplitudes were always kept below 0.1 mT (pp). K-band EPR spectra were recorded using a home-built spectrometer in the Department of Physics and Astronomy, Georgia State University, as described in detail in many previous publications.[9]

g-Tensors for **R1** and **R2** were extracted from single-crystal spectra at Q-band, recorded by rotating the crystals about the three crystallographic axes. A modified version of the program MAGRES[19,20] was used for data reduction, as previously described.[21] For **R2**, the two Schonland alternatives[22] were undistinguishable within experimental error, whereas for **R1** the one fitting best with the previous results[9] was chosen.

EPR spectrum simulations were made using the program KVASAT previously described[10] with spectral parameters from previously published work[9] or extracted as described in the text. Fitting composite spectra to experimental spectra, linear least-squares regression routines of MS EXCEL 2000 were used, producing as fitting parameters the percentage contribution of each component to the spectrum and the r^2-factor of the fitting. [Note: $r^2 = 1 - [\sum(y_i - \hat{y}_i)^2]/(\sum y_i^2 - \sum y_i^2/n)$, where $\hat{y}_i$ represents a calculated (estimated) spectrum amplitude value, n is the number of values (spectrum resolution), y_i is the

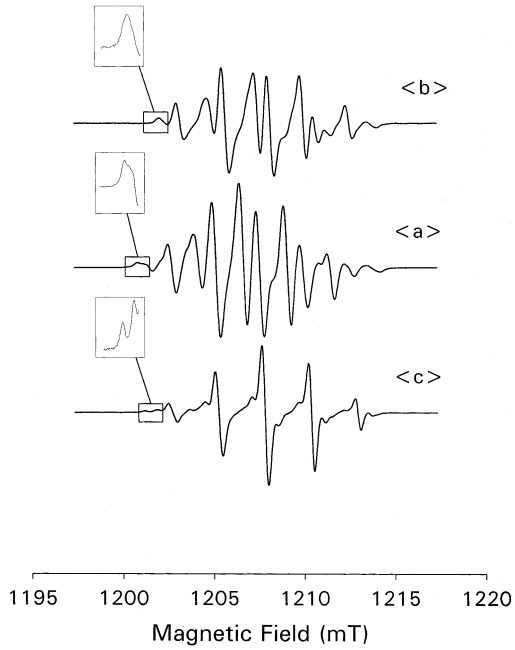

Figure 2. First derivative single-crystal Q-band EPR spectra of *l*-α-alanine recorded at 295 K with the magnetic field directed along each of the three crystallographic axes. Features specific for the **R2** radical are highlighted by insets at the low-field line positions. Microwave frequencies are 33845.77, 33900.86, and 33902.65 MHz from top to bottom.

TABLE 1: *g*-Tensors for the R1 and R2 Radicals in X-Irradiated *l*-α-Alanine at 295 K as Determined by Q-band EPR Measurements

radical	isotropic value	principal values	eigenvector ⟨*a*⟩	eigenvector ⟨*b*⟩	eigenvector ⟨*c*⟩
R1	2.0033	2.0043	0.7148	0.1057	0.6913
		2.0038	0.5546	−0.6878	−0.4683
		2.0021	0.4260	0.7181	−0.5503
R2	2.0030	2.0038	−0.1191	−0.0627	0.9980
		2.0032	0.7502	0.6593	0.0501
		2.0022	0.6611	−0.7492	−0.0392
R1[a]	2.0033	2.0041	0.828	0.030	0.559
		2.0034	0.428	−0.678	−0.598
		2.0024	0.362	0.735	−0.574

[a] From previous X-band measurements.[9]

experimental spectrum amplitude value, and the sums run over all spectral values.] ENDOR spectra were simulated using the program ENDSIM[23] modified to optimize the speed of execution (Lund, A., private communication, 2001).

3. Results and Analyses

3.1. *g*-Tensor Determination. Figure 2 shows Q-band EPR spectra from a single crystal of alanine recorded with the magnetic field parallel to each of the three crystallographic axes. Low-field features due to the **R2** radical are shown expanded in each of the spectra. This figure is directly comparable with corresponding figures in a previous paper[9] showing spectra recorded at X-band microwave frequencies. The comparison illustrates the similarity of the *g*-tensors of the two dominating radicals **R1** and **R2**. A complete set of Q-band data obtained by rotation of the crystals about the three crystallographic axes allowed for a precise determination of the *g*-tensors for **R1** and **R2**. The *g*-tensors obtained, used in the simulations reported below, are given in Table 1. The results for **R1** agree well with the previous X-band determination.[9] The direction for the minimum *g*-tensor principal value for **R2** deviates about 25° from the expected direction of the lone electron orbital (LEO) for this radical, calculated as described previously.[9]

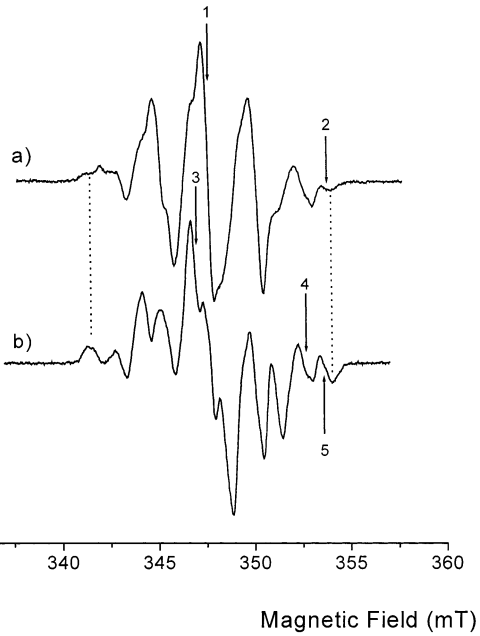

Figure 3. Effect of heating on a polycrystalline sample of *l*-α-alanine, X-irradiated at 295 K to a dose of 63 kGy. (a) X-band first derivative EPR spectrum recorded at 295 K immediately after irradiation. (b) X-band first derivative EPR spectrum recorded at 295 K after heating at 480 K for 40 min. The microwave power is the same in both cases (0.5 mW), but other instrument parameters are different. The arrows marked 1−5 indicate the field positions for the ENDOR spectra in Figures 4−6.

3.2. Warming Experiments. As mentioned in the Introduction, it has been reported that upon thermal annealing above about 460 K the EPR spectra from alanine irradiated at room temperature change irreversibly. Apparently, the **R1** radical decays faster than other radicals contributing to the spectrum.[bb,16] The spectrum due to the radicals remaining after the almost complete disappearance of **R1** also seems to be similar to that observed by Wieser et al.[17] after long-term UV-irradiation of an irradiated alanine sample. Vanhaelewyn et al. suggested that the remaining spectrum mainly is due to **R2**.[16] The possibility remains, however, that this spectrum is not the pure signature of **R2**, but a spectrum due to a mixture of, e.g., **R2** and **R3**, or of successor radicals of either **R1**, **R2**, or **R3**.

In the present work, irradiated alanine samples were warmed in a furnace set at given temperatures, and measured after recooling to room temperature. By this procedure, it was found that, with a temperature of about 480 K, the conversion could be conveniently followed. After about 40 min of warming, the spectrum in Figure 3b was obtained and is compared with the spectrum from an untreated sample (Figure 3a). [Note: The two spectra in Figure 3 are quantitatively not directly comparable, because different cavities and instrument settings were used for their recording.] The spectrum in Figure 3b is similar to those published previously.[16] The loss of spectral intensity is considerable by this procedure; the integrated area of the resonance is reduced by typically a factor of about 10 whereas the peak-to-peak amplitude value is reduced by typically a factor of 40. As indicated by the dotted lines in Figure 3, it is clear that the outer features of the resonance remaining after warming agree closely with corresponding features of the standard room-temperature alanine powder spectrum.

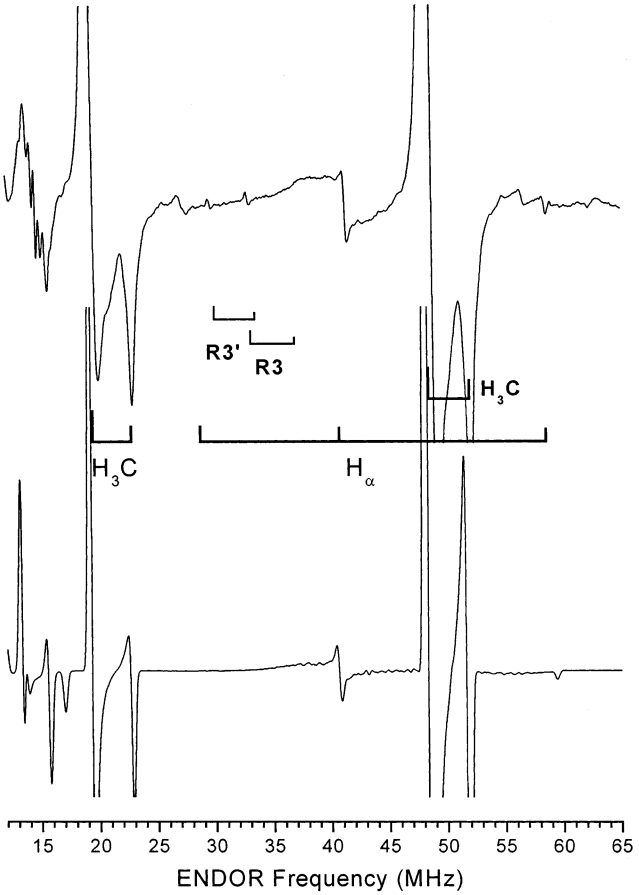

Figure 4. Experimental (top) and simulated powder ENDOR spectrum due to radical **R1** at 220 K. The experimental spectrum was obtained by saturating the central EPR resonance line (position 1, Figure 3a) at 220 K. The stick spectra represent the assigned hyperfine-coupling tensor principal values as deduced from the previous single-crystal study for radicals **R1** and **R3**. Other weak (unmarked) resonance features are due to radical **R2**, as shown in Figure 5.

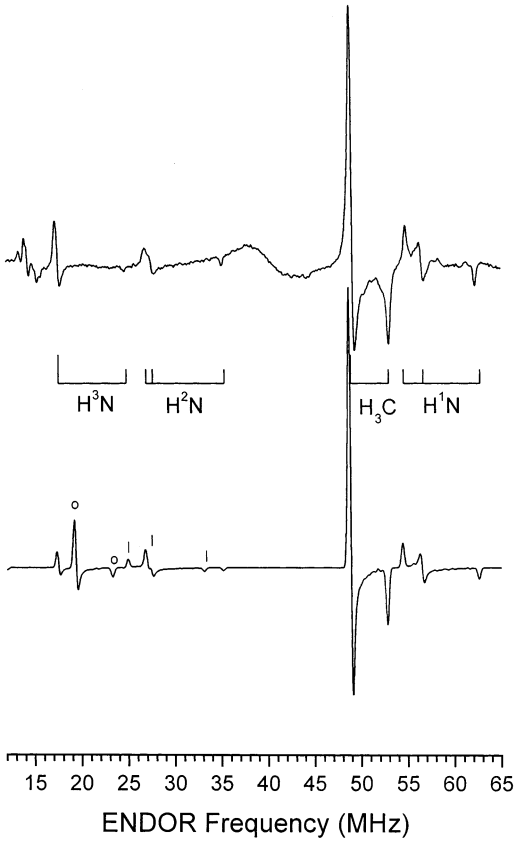

Figure 5. Experimental (top) and simulated powder ENDOR spectrum due to radical **R2** at 220 K. The experimental spectrum was obtained by saturating the very high-field EPR resonance line (position 2, Figure 3a), assumed due to **R2** only. The stick spectra represent the assigned hyperfine-coupling tensor principal values as deduced from the previous single-crystal study. In the simulated spectrum (bottom) the lines marked with o and | are the low-frequency branches of the CH_3 and H^1N ENDOR transitions, respectively. These are not observable in the experimental spectrum presumably because of relaxation effects.

3.3. Powder ENDOR. ENDOR spectra were recorded from the irradiated unwarmed and warmed polycrystalline samples. It is known[9] that the ENDOR response of the amino protons in radical **R2** is strongly temperature dependent and the temperature should be lowered to about 225 K or colder for optimum detection of these proton interactions. On the other hand, cooling the irradiated alanine sample below about 200 K results in hindrance of the free rotation of the methyl groups in both **R1** and **R2.**[9,24] Consequently, ENDOR spectra were recorded at about 220 K to optimize the ENDOR detection of the various couplings of the radicals present without introducing spectral changes due to restricted methyl rotation effects.

Figure 4 (top) shows the ENDOR spectrum recorded at 220 K from an alanine sample, X-irradiated at 295 K to a dose of 63 kGy. The magnetic field was locked to the center line of the corresponding EPR resonance in Figure 3a (marked by numeral 1). The stick spectra in Figure 4 indicate the expected line positions for radicals R1 and the two conformations of **R3** as calculated from the principal values of the hyperfine coupling tensors for these radicals.[9] For both radicals, the agreement between the experimental and predicted line positions generally is very good. However, the minimum principal value of the α-proton hyperfine coupling tensor for **R1** experimentally seems to be poorly expressed at this value of the locked magnetic field. This is further demonstrated by the simulated ENDOR spectrum due to the **R1** radical alone shown in the bottom part of the figure. This simulation was also obtained using previously published[9] tensor parameters for **R1**. Other resonance features in Figure 4 are due to radical **R2**, as shown below.

Figure 5 (top) shows the ENDOR spectrum recorded at 220 K, locking the magnetic field to the position marked with numeral 2 in Figure 3a. Apparently, no resonance features due to radicals **R1** and **R3** are present. The resonance features observed are those due to the methyl group and the three amino protons of **R2**. Line positions expected for **R2** based on the single-crystal data[9] (recalculated to the current magnetic field value) are indicated by stick spectra, similar to those in Figure 4. In the lower part of Figure 5, the corresponding simulated powder ENDOR spectrum due to the **R2** radical alone is shown. It is important to be aware that in the experimental spectra, the low-frequency branch of the different couplings does not contribute at this EPR spectral position presumably because of relaxation effects, as previously discussed.[9] The simulation program does not include relaxation effects. Thus, lines marked with | (low-frequency H^1**N** coupling) and o (low-frequency methyl coupling) in the spectra are not observed experimentally.

After thermal annealing of the X-irradiated alanine samples at 480 K for 40 min, the EPR spectrum in Figure 3b is obtained. In Fig. 6a−c are shown the ENDOR spectra obtained (at 220 K) by locking the magnetic field to the three positions marked by numerals 3−5 in Figure 3b, respectively. The stick spectra included in Figure 6 are those for the major hyperfine couplings

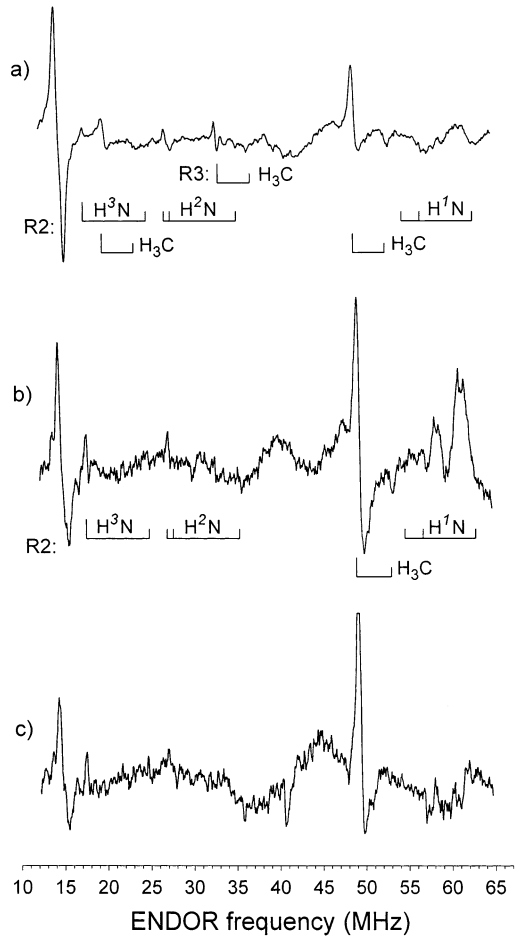

Figure 6. (a) Experimental powder ENDOR spectrum at 220 K obtained by saturating almost-center EPR resonance line (position 3, Figure 3b) obtained after 40-min warming of the X-irradiated sample at 480 K. The stick spectra represent the recalculated hyperfine coupling tensor principal values for the **R2** radical (high-frequency branches only), as deduced from the previous single-crystal study, for the present magnetic field position. (b) As above, with magnetic field locked to position 4 in Figure 3b. (c) As above, with magnetic field locked to position 5 in Figure 3b.

of radical **R2**, similar to those in Figure 5, as well as for one of the **R3** conformations. It is noted that the ENDOR is very weak and despite many efforts we were not able to obtain experimental spectra with better S/N ratios that those presented here.

The ENDOR spectrum in Figure 6a was recorded with the magnetic field at a central position. Thus, both high- and low-frequency branches of the various hyperfine couplings of **R2** should be detectable together with the **R3** resonance, which also saturated at this position. **R1,** which has decayed, should not contribute resonance features to these spectra. Figure 6a indeed shows a prominent feature due to radical **R3** (the unmarked conformation[9]). Similarly, clear features due to the methyl coupling of **R2** (both high- and low-frequency branches) are observed at this magnetic field value together with at least two of the three amino proton couplings. The ENDOR spectra in Fig. 6b,c were recorded with the magnetic field locked to extreme field positions (positions 4 and 5 in Figure 3b) where neither the **R3** resonance nor the low-frequency branch of the **R2** couplings are expected to contribute (relaxation effects). Again, the methyl coupling and at least two of the three amino proton couplings of **R2** are easily recognized, whereas the largest amino proton coupling of **R2** is only barely observable. None of the spectra display any features due to **R1**.

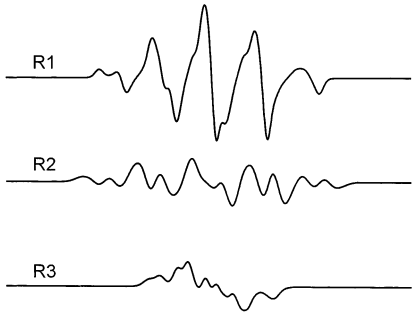

Figure 7. Simulated polycrystalline EPR spectra for the three radicals **R1**−**R3** formed in *l*-α-alanine after X-irradiation at 295 K. The parameters used for these simulations are described in the text for **R1** and **R2**, and in Table 3 for **R3**. These three spectra have been used as the basis spectra for all simulations shown in Figures 8−10.

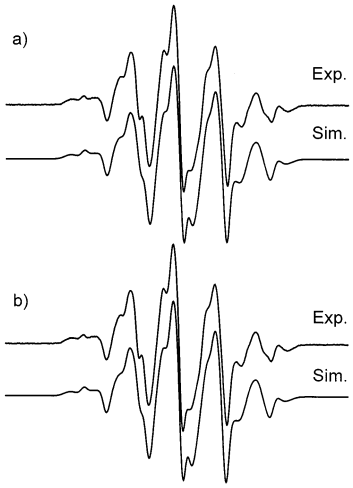

Figure 8. Simulated X-band EPR spectra from polycrystalline *l*-α-alanine obtained after X-irradiation (dose = 60 kGy) at room temperature. In both a and b, the experimental spectrum is shown as the top trace and the simulated spectrum as the bottom trace. All final fitting parameters are given in Table 2. (a) Spectrum reconstructed using **R1** and **R2**. (b) Spectrum reconstructed using **R1**, **R2**, and **R3**.

Considering the total width of the EPR spectra in Figure 3, and the clear detection of the methyl coupling and at least two of the three amino proton couplings of radical **R2** in Figure 6, there can be no doubt that radical **R2** is present in its original form even after prolonged warming to 480 K. Furthermore, these ENDOR spectra yield evidence that the **R3** radical (unmarked conformation) also contributes to the total resonance after annealing at 480 K.

3.4. EPR Spectrum Simulations. The first goal with respect to spectrum simulations is to obtain a satisfactory simulation of the room-temperature EPR spectrum from polycrystalline *l*-α-alanine, based on the resonance parameters for **R1** and **R2**, eventually also including **R3**. For that purpose, the *g*-tensors in Table 1 were used, together with published hyperfine coupling parameters for **R1** and **R2**.[9] Only the nitrogen hyperfine-coupling tensor of radical **R2** is not known. However, the estimate previously made[9] was used. The two top spectra of Figure 7 show each of the simulated spectra of **R1** and **R2**, normalized to unit area. These simulated spectra were subsequently added to best fit the experimental spectrum using regular regression routines in MS EXCEL. Figure 8a shows the result of the fitting, with the fitted spectrum shown as the lower trace and the experimental spectrum as the top trace. The relative weight (by integrated area) of the two components in the final spectrum was **R1**, 63.5%; **R2**, 36.5%, with the r^2 factor being

TABLE 2: Fitting Parameters for the Simulated Spectra in Figures 8−10

system description	regression factor (r^2)	radical	weight
X-band, 295 K	0.979	**R1**	0.635
R1 + **R2**		**R2**	0.365
(Figure 8a)			
X-band, 295 K	0.980	**R1**	0.589
R1 + **R2** + **R3**		**R2**	0.335
(Figure 8b)		**R3**	0.076
X-band, 480/295 K	0.690	**R1**	0.112
R1 + **R2**		**R2**	0.888
(not shown)			
X-band, 480/295 K	0.961	**R1**	0.061
R1 + **R2** + **R3**		**R2**	0.507
(Figure 9)		**R3**	0.432
K-band, 295 K	0.959	**R1**	0.594
R1 + **R2** + **R3**		**R2**	0.322
(Figure 10a)		**R3**	0.084
Q-band, 295 K	0.953	**R1**	0.579
R1 + **R2** + **R3**		**R2**	0.379
(Figure 10b)		**R3**	0.042

TABLE 3: Spectral Parameters Used for the Simulation of EPR Spectra from Radical R3 in X-Irradiated Alanine at 295 K (Hyperfine Couplings in MHz)

	spectral parameter			
	g [a]	A[CH_3] [b]	A[N_β] [c]	A[H(N_β)] (2) [d]
principal values	2.0040	44.5	11.2	−25.2
	2.0030	37.3	−8.4	−16.8
	2.0020	36.8	−5.6	0.0

[a] Eigenvectors along the C═O bond direction (maximum value), normal to the plane N−C_α−C (minimum value) and perpendicular to these two directions (intermediate value). [b] Eigenvectors from ref 9 exhibiting a maximum value along the C_α−CH_3 bond direction. [c] Eigenvectors along the normal to the plane N−C_α−C (numerically largest value), the N−C_α bond direction (intermediate value), and perpendicular to these two directions (numerically smallest value). [d] Eigenvectors along the normal to the plane N−C_α−C (intermediate value), each of the two N−H bond directions (numerically smallest value), and perpendicular to these directions (numerically largest value).

0.979. This agrees well with the estimates of the composition of single-crystal spectra made previously.[9] All fitting parameters for the simulations made in the present paper are summarized in Table 2.

It is clear from previous results,[9] however, that the experimental spectrum at room temperature consists of resonances from more than two radicals. Radical **R3** is poorly characterized experimentally and only the methyl hyperfine-coupling tensor for two conformations of this radical is known. The ENDOR spectrum in Figure 6 suggests that the conformation exhibiting the largest methyl hyperfine coupling is dominating after warming and in the following text only this conformation of **R3** is taken into consideration. Additional parameters for **R3** were constructed on the basis of previously published parameters from similar radicals.[25−27] These parameters are listed in Table 3. Figure 7c shows the calculated spectrum obtained using these parameters, normalized to unit area. Figure 8b shows the simulated spectrum obtained using these parameters for the dominating conformation **R3** together with the theoretical spectra for **R1** and **R2**. The relative contributions from the different radicals are **R1**, 0.589; **R2**, 0.335; and **R3**, 0.076. For this simulation, the r^2 factor is $r^2 = 0.980$.

As described above, after warming at temperatures above 460 K, the spectrum changes in that **R1** apparently decay faster than **R2** and **R3**. The top spectrum of Figure 9 is the same as that in Figure 3b, representing the spectrum obtained after warming at 480 K for 40 min. Now, using the basis spectra in Figure 7 for **R1**, **R2**, and **R3**, this spectrum was successfully simulated as demonstrated by the lower trace in Figure 9. For this simulation, the relative contributions to the spectrum are **R1**, 0.061; **R2**, 0.507; and **R3**, 0.432, with $r^2 = 0.961$. When an attempt was made to simulate the spectrum with **R1** and **R2** only (not shown), the r^2 factor dropped significantly to 0.690. This result thus clearly shows that **R3** is an important part of the resonance observed after thermal annealing, and also that the **R1** resonance still contributes slightly after 40 min at 480 K.

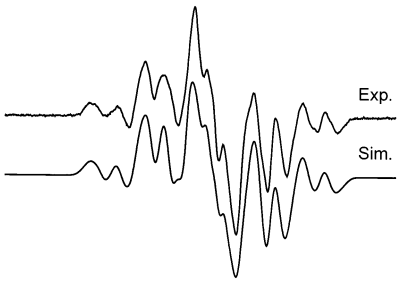

Figure 9. Simulated X-band EPR spectra from polycrystalline *l*-α-alanine obtained after X-irradiation at room temperature (dose = 63 kGy) followed by warming at 480 K in 40 min, measured at room temperature. The experimental spectrum is shown as the top trace, and the reconstructed spectrum using the basis spectra for all radicals R1−**R3** in Figure 7 is shown as the bottom trace. All final fitting parameters are given in Table 2.

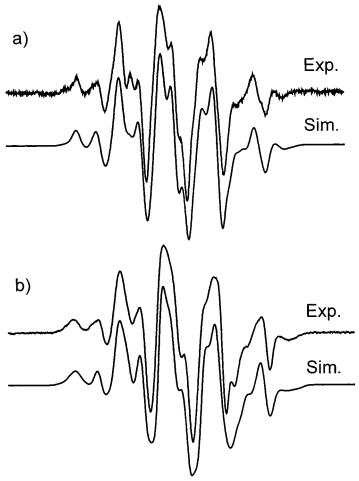

Figure 10. Simulated EPR spectra from polycrystalline *l*-α-alanine obtained after X-irradiation at room temperature. The experimental spectra are shown as the top trace and the simulated as the bottom trace. All experimental spectra were reconstructed using the basis spectra for the three radicals **R1**−**R3** shown in Figure 7. All final fitting parameters are given in Table 2. (a) K-band (24 GHz) EPR spectrum at room temperature; dose, 10 kGy. (b) Q-band (34 GHz) EPR spectrum at room temperature, dose, 63 kGy.

Figure 10 shows experimental and simulated EPR spectra for polycrystalline alanine X-irradiated at 295 K recorded at (Figure 10a) K-band and (Figure 10b) Q-band microwave frequencies. All experimental spectra were recorded at 295 K. Although these simulations resulted in r^2 factors slightly smaller than those for the previous simulations, most features of the experimental spectra apparently are reproduced satisfactorily.

4. Discussion

The results presented above clearly show that the **R2** radical has a significant contribution to the EPR spectra obtained from polycrystalline X-irradiated *l*-α-alanine at room temperature as

well as after warming to 480 K for 40 min. At room temperature, the estimated contribution of **R2** (≈35%) agrees well with similar estimations from single-crystal spectra.[9]

A third resonance, due to radical **R3**, contributes to the spectra at all temperatures at or above room temperature. At room temperature, the contribution is relatively small (5−10%) whereas after warming at 480 K the relative contribution is far larger, on the order of 40%. On the other hand, the **R1** radical seems to be practically absent in thermally annealed samples, whereas this is the dominating species (≈55%) at room temperature.

The quantitative estimates are based on simulations of the EPR spectra of the three components. They must be considered as approximate for a variety of reasons. First, the parameters used for the simulations are not exactly known for all the species. For **R2**, a nitrogen-hyperfine interaction has been estimated. For **R3**, all hyperfine interactions except for the methyl coupling, as well as the *g*-tensor are estimated. For all three radicals, the line-width variations with radical orientation have not been taken into account; it has been assumed that the line widths are isotropic. For **R2**, the lack of a precisely known nitrogen-hyperfine interaction combined with an isotropic line-width tensor may result in differences between the experimental and simulated spectra. This is particularly visible in Figure 10. For **R3**, on the other hand, the simulated spectra can be no more than an approximate representation of the actual spectrum. An indication of this was obtained by calculating a difference spectrum between the experimental spectrum obtained after annealing at 480 K and a sum of **R1** and **R2**, fitted to the outer part only of the experimental spectrum. The spectral width of the simulated **R3** spectrum and this difference spectrum agreed nicely as did the overall shape of the resonance, but the detailed hyperfine structure of the difference spectrum was only partly reproduced by the simulated spectrum.

Several attempts have been made to isolate the **R2** and **R3** components experimentally. This would have been particularly helpful for confirming the suggested structure of **R3**, and also for estimating the spectral parameters of **R3** for simulation purposes. However, ENDOR-induced EPR spectra never yielded sufficiently strong signals to reveal the **R3** resonance above the noise level. Field-swept electron spin−echo spectroscopy is another method with the potential of separating radical components with different relaxation times.[28] During the present work, attempts were made to use field-swept electron spin−echo techniques to isolate **R2** and **R3**. However, the experiments showed that the relaxation times for the three radicals in alanine are fast (T_M's of the order of 130 ns, in general agreement with previous work[29,30]), and not sufficiently different for separating the spectral components. Hence, no reliable experimental view of the **R3** resonance is presently available.

The parameters used for the **R3** simulation are, with one exception, in good agreement with those calculated using DFT methods.[12,13,31] The one exception is the nitrogen-hyperfine interaction. Although DFT methods predict a very anisotropic nitrogen interaction, this is not in agreement with our analysis of the **R3** resonance, nor with experimental data for several similar radicals with an N−H fragment in α-position to a carbon with large 2π-spin density for which similar discrepancies were found.[25−27]

The **R3** radical is a significant contributor to the EPR spectra obtained after annealing at 480 K. Thus, the collected data indicate that the three radicals in alanine have a very different stability at elevated temperatures. Preliminary measurements have indicated that **R1** is reduced by a factor of about 80, **R2** by a factor of about 8, and **R3** by a factor about 2, comparing spectra obtained immediately after irradiation at room temperature with those obtained after warming at 480 K for 40 min, measured at room temperature. The detailed kinetics of these radical decay processes will be discussed elsewhere.

Acknowledgment. We are grateful to Professor Anders Lund, Linköping, Sweden, for providing the simulation programs used in this work and for his help with the ENDOR simulations, and together with Dr. Marco Bonora for helping with performing FT-EPR measurements on alanine. Professor William H. Nelson, Atlanta, GA, is acknowledged for providing the MAGRES program used for single-crystal spectral analyses as well as for using his K-band EPR/ENDOR spectrometer. We also thank Professor Bartlomiej Ciesielski, Gdansk, Poland, for stimulating discussions. This work was supported in part by National Institutes of Health Grant CA 36810.

References and Notes

(1) Bradshaw, W. W.; Cadena, D. G.; Crawford, G. W.; Spetzler, H. A. W. *Radiat. Res.* **1962**, *17*, 11.
(2) Regulla, D. F.; Deffner, U. *Appl. Radiat. Isot.* **1982**, *33*, 1101.
(3) Nam, J. W.; Regulla, D. F. *Appl. Radiat. Isot.* **1989**, *40*, 953.
(4) Ciesielski, B.; Wielopolski, L. *Radiat. Res.* **1994**, *140*, 105.
(5) Miyagawa, I.; Gordy, W. *J. Chem. Phys.* **1960**, *32*, 255.
(6) Morton, J. R.; Horsfield, A. *J. Chem. Phys.* **1961**, *35*, 1142.
(7) Kuroda, S.-I.; Miyagawa, I. *J. Chem. Phys.* **1982**, *76*, 3933.
(8) Arber, J. M.; Sharpe, P. H. G.; Joly, H. A.; Morton, J. R.; Preston, K. F. *Appl. Radiat. Isot.* **1991**, *42*, 665.
(9) Sagstuen, E.; Hole, E. O.; Haugedal, S. R.; Nelson, W. H. *J. Phys. Chem. A* **1997**, *101*, 9763.
(10) Sagstuen, E.; Hole, E. O.; Haugedal, S. R.; Lund, A.; Eid, O. I.; Erickson, R. *Nukleonika* **1997**, *42*, 353.
(11) Bugay, A. A.; Onischuk, V. A.; Petrenko, T. L.; Teslenko, V. V. *Appl. Radiat. Isot.* **2000**, *52*, 1189.
(12) Petrenko, T. L. *J. Phys. Chem. A* **2002**, *106*, 149.
(13) Ban, F.; Wetmore, S. D.; Boyd, R. J. *J. Phys. Chem. A* **1999**, *103*, 4303.
(14) Lahorte, P.; De Proft, F.; Vanhaelewyn, G.; Masschaele, B.; Cauwels, P.; Callens, F.; Geerlings, P.; Mondelaers, W. *J. Phys. Chem. A* **1999**, *103*, 6650.
(15) Pauwels, E.; Van Speybroeck, V.; Lahorte, P.; Waroquier, M. *J. Phys. Chem. A* **2001**, *105*, 8794.
(16) Vanhaelewyn, G. C. A. M.; Mondelaers, W. K. P. G.; Callens, F. J. *Radiat. Res.* **1999**, *151*, 590.
(17) Wieser, A.; Lettau, C.; Fill, U.; Regulla, D. F. *Appl. Radiat. Isot.* **1993**, *44*, 59.
(18) Lehmann, M. S.; Koetzle, T. F.; Hamilton, W. C. *J. Am. Chem. Soc.* **1972**, *94*, 2657.
(19) Nelson, W. H.; Gill, C. *Mol. Phys.* **1978**, *36*, 1779.
(20) Nelson, W. H. *J. Magn. Reson.* **1980**, *38*, 71.
(21) Sagstuen, E.; Lund, A.; Itagaki, Y.; Maruani, J. *J. Phys. Chem. A* **2000**, *104*, 6362.
(22) Schonland, D. S. *Proc. Phys. Soc. London, Sect. A* **1959**, *73*, 788.
(23) Lund, A.; Erickson, R. *Acta Chem. Scand.* **1998**, *52*, 261.
(24) Itoh, K.; Miyagawa, I. *J. Mol. Struct.* **1988**, *190*, 85.
(25) Sanderud, A.; Sagstuen, E. *J. Phys. Chem. B* **1998**, *102*, 9353.
(26) Salih, N. A.; Sanderud, A.; Sagstuen, E.; Eid, O. I.; Lund, A. *J. Phys. Chem. A* **1997**, *101*, 8214.
(27) Hosseini, A.; Lund, A.; Sagstuen, E. *Phys. Chem. Chem. Phys.* **2002**, submitted for publication.
(28) Schweiger, A.; Jeschke, G. *Principles of Pulse Electron Paramagnetic Resonance*; Oxford University Press: New York, 2001.
(29) Höfer, P.; Holczer, K.; Schmalbein, D. *Appl. Radiat. Isot.* **1989**, *40*, 1233.
(30) Nakagawa, K.; Eaton, S. S.; Eaton, G. R. *Appl. Radiat. Isot.* **1993**, *44*, 73.
(31) Ban, F.; Gauld, J. W.; Boyd, R. B. *J. Phys. Chem. A* **2000**, *104*, 5080.